IEEE Access
Multidisciplinary ⁝ Rapid Review ⁝ Open Access Journal

Received 23 December 2022, accepted 13 January 2023, date of publication 26 January 2023, date of current version 3 February 2023.

Digital Object Identifier 10.1109/ACCESS.2023.3240065

RESEARCH ARTICLE

Game Theory Based Delta-OMA Scheme for VLC Networks

PRIYASHANTHA TENNAKOON[1,2], (Member, IEEE), SAMIKKANNU RAJKUMAR[2], (Member, IEEE), AND DUSHANTHA NALIN K. JAYAKODY[1], (Senior Member, IEEE)

[1]COPELABS, Lusófona University, 1749-024 Lisbon, Portugal
[2]Center for Telecommunication Research, School of Engineering, Sri Lanka Technological Campus, Padukka 10500, Sri Lanka

Corresponding author: Dushantha Nalin K. Jayakody (dushantha.jayakody@ulusofona.pt)

This work was supported in part by the Fundação para a Ciência e a Tecnologia, Portugal, under Grant UIDB/04111/2020 (COPELABS) and Grant 2022.03897.PTDC; and in part by the University of Lusófona under Grant COFAC/ILIND/COPELABS/2/2022.

ABSTRACT This paper proposes a delta-orthogonal multiple access (D-OMA) scheme-based visible light communications (VLC) network to enhance spectral efficiency and massive connectivity in the indoor environment. The D-OMA scheme is an advanced version of the non-orthogonal multiple access (NOMA) scheme. D-OMA allows the partial overlapping of the in-band NOMA clusters to achieve the benefits of a massive in-band NOMA scheme with low power consumption and less complexity. In this work, the massive in-band NOMA scheme is used as a special case of the proposed D-OMA scheme. Game theory is employed for the user grouping mechanism, which enhances the sum rate of the proposed network. Closed-form expressions for the bit error rate (BER) and outage probability of the proposed network are derived. Further, downlink transmission power optimization is performed using Karush-Kuhn Tucker (KKT) conditions to improve the outage performance of the proposed D-OMA VLC network. The presented numerical results show the effect of optical filter gain and field of view (FoV) in indoor communication. Further, it is noted that the BER performance of the D-OMA scheme outperforms the massive in-band NOMA scheme due to the cluster sizes which control the interference in the D-OMA scheme. Moreover, the sum rate of the proposed network is significantly improved using the preference relation algorithm (PRA) compared to the random NOMA scheme.

INDEX TERMS Delta-orthogonal multiple access, massive in-band NOMA, visible light communications.

I. INTRODUCTION

In recent wireless multi-media communications, mobile data usage grows exponentially without limits which leads to the scarcity in the radio spectrum of future wireless networks. Further, due to the rapid development of the internet of things (IoT) and other low-power wireless networks, the demand for massive access to nodes increases in various wireless networks. In this scenario, the concept of optical wireless communication (OWC) is proposed to improve the spectrum usage and massive accessibility in wireless networks such as e-healthcare, e-transport, industrial automation, etc [1]. Moreover, the optical network design with nested small cells such as femtocells and attocells will further enhance the accessibility of wireless networks. Visible light (VL) has several unique features, which include hundreds of Terahertz of unlicensed bandwidth, the capability of isolation due to prevention from penetration into objects or walls, secure communications etc [2].

Interestingly, the existing light-emitting diodes (LEDs) support well in optical transmission due to their high-speed switching rate. In particular, white LED is considered as a primary candidate for future lightwave technology due to its long lifetime, low power consumption, and high brightness [3]. In addition, LEDs' average luminous efficacy (113 lumens/ watts) and lifespan (from 25,000 to 50,000 hours) period guarantee the quality of service (QoS) of visible light communication (VLC). Also, the frequency response of

The associate editor coordinating the review of this manuscript and approving it for publication was Tiago Cruz.

white LED is an essential factor to consider in VLC communication. In [4] the frequency response of UXEON3020 LED has been measured and shows low pass characteristics with a 3 dB bandwidth of 1.47 MHz. Moreover, the DC bias current of a VLC transmitter affects the magnitude of the frequency response. The magnitude of the frequency response reduces with the reduction of the DC bias current. Whereas the magnitude of the frequency response increases with the DC bias current at a higher frequency due to the higher optical power detected at the receiver.

In fact, the VLC technique has several advantages when compared to RF communication. For instance, it has high spatial reuse characteristics due to its signal isolation which provides secure communication. Since the VLC is a non-coherent communication system, the transmit and receive front-ends do not require many complex signal processing units, unlike the RF receiver circuits. Inherently, VLC networks achieve a high data rate due to the large Terahertz spectrum, and it operates with simple transmission techniques such as intensity modulation/direct detection (IM/DD). In the recent surveys, it was identified that many of the people and their services mainly depend on the indoor environment; therefore, VLC will be a more demanded one in the upcoming year [5].

It is noteworthy that the Doppler effect does not exhibit in the VLC channel. Hence it is easy to model as a time-invariant channel in the indoor environment [6]. For the given setup, such as room shape, user/node location, and light source type, the VLC channel is simply modeled as a deterministic direct current (DC) channel. Further, VLC signals inherently provide a high signal-to-noise ratio (SNR) due to their dominant line of sight (LOS) path and short distances of users/nodes [7]. However, the VLC links can also be modeled using the reflections, refraction, and diffusion components [8].

The main challenges in the VLC networks arise from the fact of limitation of the modulation bandwidth with respect to the LED characteristics. Hence VLC support only a limited data rate. In this scenario, the multiple access (MA) scheme is identified as a suitable method to enhance the data rate of the VLC networks. In particular, frequency division multiple access (FDMA) and orthogonal frequency division multiple access (OFDMA) is the preferred multiple access schemes to achieve high spectral efficiency in the VLC networks. However, these multiple access techniques have limitations, such as the DC biasing and signal clipping requirement to convert the signal values as real and non-negative [9]. Therefore, VLC networks need a new promising multiple access scheme requirement to enhance their performance.

A. REVIEW ON MULTIPLE ACCESS TECHNIQUES IN VLC

An optical OFDM scheme is initially employed in the VLC networks to achieve a high data rate. However, it leads to the peak-to-average power ratio (PAPR) problem due to the non-linearity behavior of the LEDs [10]. Hence, the single carrier frequency division multiple access (SC-FDMA) scheme is proposed for the VLC network [11], which significantly reduces the PAPR level. Basically, SC-FDMA can be modeled as a fast-Fourier transform (FFT) precoded OFDM scheme, which achieves the benefits of OFDMA. In fact, SC-FDMA outperforms the OFDMA scheme due to the frequency diversity gain [12]. However, the joint equalization process in the SC-FDMA scheme is the critical one that increases the receiver complexity [13]. On the other hand, OFDMA supports dynamic resource allocation and scheduling. Hence it works well on the medium access control (MAC) protocol [14]. Practically, OFDMA is used in the long-term evaluation (LTE) downlink and SC-FDMA is used in the LTE uplink.

Recently, a new multiple access scheme known as the non-orthogonal multiple access (NOMA) scheme has been proposed for RF-based fifth-generation (5G) wireless networks to improve spectral efficiency and massive connectivity. Generally, the NOMA scheme is easily adopted with downlink transmission [15], [16]. However, the end-to-end transmission of the NOMA wireless network is established by combining the physical-layer network coding (PLNC) scheme as in [17] and [18]. Inherently, the NOMA scheme is well suited for the VLC networks due to the quality of channel state information (CSI), which makes successive interference cancellation (SIC) operations more flexible. Therefore, the NOMA scheme is highly recommended for the VLC networks.

In the NOMA scheme, getting a perfect SIC operation is practically difficult because there will be a SIC residual error leading to an error propagation to the successive symbols. In this scenario, an adaptive modulation scheme based on NOMA-VLC networks is proposed as in [19], which gives SIC-free operation with respect to the channel conditions. Further, in the NOMA scheme, users are ordered based on channel conditions, and this ordering can be used for decoding, power allocation, and grouping. In the realistic wireless environment, CSI information is not always perfect, and therefore, it introduces CSI errors which will degrade the performance of the VLC networks. In such a scenario, the performance of the NOMA-VLC networks is improved using hybrid RF/VLC links [20].

Moreover, power optimization is another way to improve the performance of the NOMA wireless networks [21]. Particularly, optimal power allocation at the base stations (BS) or access points (AP) will enhance the sum rate of the NOMA-VLC networks under LED light constraints [22]. Mostly, on-off keying (OOK) modulation is preferred in the VLC networks [23] due to its easy implementation with LED. However, in [24] and [25], higher-order modulation is also considered to improve the reliable data rate in the VLC networks.

B. REVIEW ON CLUSTERING IN VLC

User clustering in NOMA-based wireless networks is another challenging issue and using such suitable clustering algorithms the sum rate of the NOMA wireless network is significantly improved. In this direction, the game theory approach to employed for user clustering in NOMA wireless network to enhance the sum rate [26]. User grouping using the preference relation algorithm (PRA) is proposed for the NOMA wireless networks, and the Shapley value is calculated to allocate the payoff to each user such that the sum rate is improved in the VLC network [27]. Also, low complexity sub-optimal user clustering algorithm is proposed for uplink and downlink NOMA systems using channel gain differences in [28]. Further, the system capacity of the device-to-device VLC network is improved by selecting the optimum communication mode using the game theory approach in [29]. Similarly, user grouping in the VLC networks is performed based on the user's location in [30]. Therefore, the game theory-based VLC networks with the D-OMA scheme is the promising optical wireless network model and will fill the gap in the existing indoor wireless networks.

C. MOTIVATION

In the future, it is expected that new multiple access schemes with white LED sources will brighten the VLC technology. Moreover, multiplexing and micro LEDs can play a vital role in upcoming VLC wireless networks [31]. Significant requirements of sixth-generation (6G) communication include ubiquitous mobile ultra-broadband (uMUB), ultra-high-speed with low-latency communications (uHSLLC), massive machine-type communications (mMTC), and ultra-high data density (uHDD). Power-domain NOMA solves the small bandwidth modulation problems in the VLC networks. Thereby, it achieves a high data rate in indoor communication. However, the NOMA scheme has some drawbacks, such as the SIC complexity and power allocation problem. Therefore, VLC networks need an advanced multiple access scheme beyond the NOMA scheme to support such massive connections with less complexity and low power consumption.

More recently, another multiple access scheme called delta-orthogonal multiple access (D-OMA) schemes have been proposed for RF-based 6G wireless networks [32]. D-OMA scheme allows the partial overlapping of in-band NOMA clusters under distributed large coordinated multipoint (CoMP) environment. Similarly, in the in-band NOMA scheme, the total bandwidth is divided into a number of sub-bands, and each sub-band operates with a unique NOMA scheme. Due to the partial overlapping of the D-OMA scheme, the accessibility of the D-OMA scheme is higher when compared to the in-band NOMA scheme. Further, since the D-OMA scheme allows overlapping, it is unavoidable for the sub-bands to overlap interferences. However, it can be mitigated by reducing the cluster size without affecting the network performance.

By considering the accessibility and the rate issues in the VLC networks, in this paper, a new D-OMA scheme-based VLC network is proposed for indoor applications. It will meet one of the major requirements of the 6G networks, that is mMTC [33].

D. CONTRIBUTIONS

The main contributions of this paper are summarized as follows.

- Proposal of novel indoor VLC network model using D-OMA scheme. It supports massive access in the indoor environment with low complexity.
- Game theory-based user clustering is considered in this proposed D-OMA VLC network to enhance the sum rate.
- Transmission power optimization is performed under QoS, outage, and dimming control constraints. It ensures the QoS of all the users within the clusters.
- BER and outage probability analytical expressions of the proposed network are derived.

The remaining part of the paper is arranged as follows: In section II, the system model of the proposed D-OMA VLC network and user clustering are discussed. The achievable rates, BER and the outage probability of the proposed network are discussed in section III. Two users' cluster-based D-OMA downlink transmission is discussed in section IV. Downlink transmission power optimization of the proposed network is explained in section V. Numerical results are presented in section VI, and the concluding remarks are given in section VII.

II. SYSTEM MODEL

Consider the downlink transmission of a VLC attocell where LED is mounted on the ceiling of the room and N users are distributed uniformly inside the room as shown in the circular area (coverage area of the LED) of Fig. 1. In this model, D-OMA is applied as a special MA scheme to serve all the users simultaneously with sub-band overlapping. Basically, in the D-OMA scheme, the entire bandwidth W is divided into M number of sub-bands and partially overlapped with allowable interference. Then, each sub-band is allocated a group of users and operates with the NOMA scheme as depicted in Fig. 2. Therefore, within the allocated bandwidth, the number of users using the D-OMA scheme is greater than the non-overlapping massive in-band NOMA scheme. In this model, all the users are grouped into several subsets of users. Therefore we refer to the subset of users as a NOMA cluster. Further, the number of sub-bands is equal to the number of NOMA clusters such that each sub-band is allocated to one NOMA cluster. User grouping is performed using the coalitional game theory approach, which is discussed in detail in the next subsection. Generally, user grouping is performed by pairing the near user and the far user. Thereby, the sum rate of the wireless network can be increased [33]. Therefore, for the user grouping, we initially adopted with basic user grouping algorithm as in [33]. During the user grouping, it is assumed that the perfect CSI is known at the BS (i.e., LED transmitter) and the users, and it is modeled as a static or quasi-static.

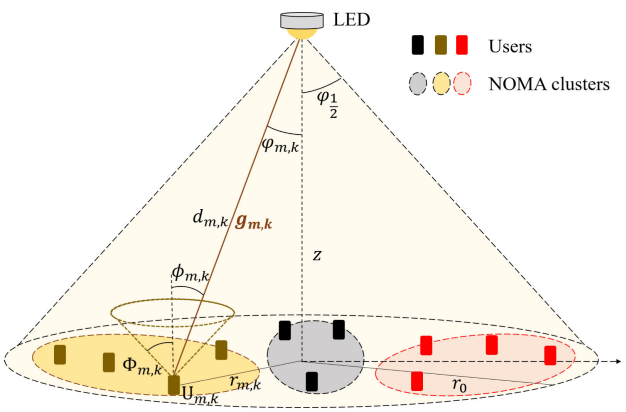

FIGURE 1. A D-OMA VLC network system.

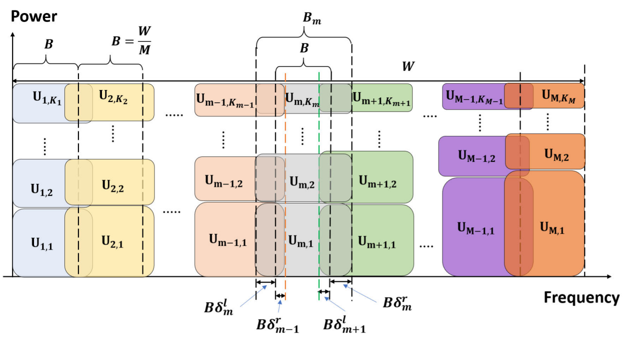

FIGURE 2. Illustration of D-OMA sub-bands and power allocation.

Each user in the sub-band $m = \{1, \ldots, M\}$ is denoted as $\mathrm{U}_{m,k}$ where $k = \{1, \ldots, K_m\}$, M is total number of sub-bands and K_m is the maximum number of users in the sub-band m. Let the bandwidth of each sub-band is $B = W/M$ and the number of overlapping portions of adjacent sub-bands for example m^{th} sub-band left and right side overlapping is $B\delta_m^l$ and $B\delta_m^r$, respectively. Therefore, the effective bandwidth of each sub-band becomes $B_m = B(1 - (\delta_m^l + \delta_m^r))$. Note that, when $\delta_m^l = \delta_m^r = 0$, the overlapped amount of sub-bands is 0 and this corresponds to massive in-band NOMA scheme thus partial overlapping inter-cluster interference (PICI) is neglected. However, when $\delta_m^l = \delta_m^r = 1$, the adjacent bands are overlapped and PICI is maximum. The allocated power to the $\mathrm{U}_{m,k}$ is denoted as $P_{m,k}$, and the power allocation is based on the channel conditions, $g_{m,k}$ of the users. Without loss generality, let us assume $g_{m,1} < g_{m,2} < \ldots, < g_{m,K_m}$, then the allocated powers becomes $P_{m,1} > P_{m,2} > \ldots, > P_{m,K_m}$.

A. OPTICAL TRANSMISSION POWER

Let us consider the transmit electrical signal at the LED is $x(t) \in (0, +1)$ for on-off keying (OOK) modulation. Then the transmitted optical signal at the BS (i.e., LED) can be given as

$$x_s(t) = P_{\text{LED}}[x(t) + I_{\text{DC}}], \tag{1}$$

where P_{LED} is the LED power at the BS in W/A, and I_{DC} is the added DC bias at the BS to obtain non-negative signals, i.e. $x(t) + I_{\text{DC}} \geq 0$. Due to the illumination and safety requirements, I_{DC} is chosen between $0 \leq I_{\text{DC}} \leq P_a$, where P_a is the permissible average optical power and $\mathbb{E}[x_s] \leq P_a$.

B. VLC CHANNEL MODEL

In this work, we assumed that the communication between the LED and a user is carried out only through the LOS path. The LOS direct current (DC) channel gain in VLC, $g_{m,k}$ from the BS to the user $\mathrm{U}_{m,k}$ is given by [2]

$$g_{m,k} = \begin{cases} \dfrac{A_{m,k}}{d_{m,k}^{\upsilon}} R_0(\varphi_{m,k})\, T(\phi_{m,k})\, G(\phi_{m,k})\, \cos(\phi_{m,k}), & 0 \leq \phi_{m,k} \leq \Phi_{m,k}, \\ 0, & \phi_{m,k} > \Phi_{m,k}, \end{cases} \tag{2}$$

where $A_{m,k}$, $\Phi_{m,k}$ and $\phi_{m,k}$, denote the photodetector (PD) area, the field of view (FoV) of the PD and the angle of incidence of the user $\mathrm{U}_{m,k}$, respectively. Further, the parameters $d_{m,k}$ is the distance from the LED to $\mathrm{U}_{m,k}$, υ is the path loss exponent, $\varphi_{m,k}$ is the angle of irradiation of the transmitter LED and $T(\phi_{m,k})$ is the gain of the optical filter. Also, the parameter $R_0(\varphi_{m,k})$ is the Lambertian radiant intensity of the LED transmitter and it can be expressed as

$$R_0(\varphi_{m,k}) = \frac{\mu + 1}{2\pi} \cos^{\mu}(\varphi_{m,k}), \tag{3}$$

where μ represents the order of Lambertian emission which is given as $\mu = -\ln(2)/\ln[\cos(\varphi_{1/2})]$, in this $\varphi_{1/2}$ denotes the transmitter LED semi-angle at half power (half irradiation) of the BS. In addition, $G(\phi_{m,k})$ is the gain of the optical concentrator of the PD and it can be expressed as $G(\phi_{m,k}) = \nu^2/\sin^2(\Phi_{m,k})$ where ν is the refractive index.

By substituting (3) into (2), LOS VLC channel gain can be expressed as

$$g_{m,k} = \frac{C(\mu + 1)\cos^{\mu}(\varphi_{m,k})\, \cos(\phi_{m,k})}{(z^2 + r_{m,k}^2)}, \tag{4}$$

where C is a constant given by

$$C = \frac{1}{2\pi} A_{m,k}\, T(\phi_{m,k})\, G(\phi_{m,k}), \tag{5}$$

C. USERS CLUSTERING: COALITIONAL GAME APPROACH

In this section, user clustering within each sub-band of the VLC network is discussed. Users are clustered according to their channel conditions such that the sum rate of the proposed network is enhanced. It is noted that users are cooperative with each other within the cluster using the NOMA scheme. Each user has a non-transferable utility (NTU), and it is treated as a random NOMA. Further, the orthogonal multiple access (OMA) scheme is used if only one user is located inside the cluster.

Consider there is N number of users distributed in the attocell and form the M coalitions. Therefore, the number of coalitions is equal to the number of sub-bands. Let C be the initial coalitions of this game, and the sum of the cardinality of all the coalitions is equal to N. Each coalition within the attocell can satisfy the condition as given by

$$\mathrm{C}_i \cap \mathrm{C}_j = \emptyset, \forall i, j \leq M,\ i \neq j, \tag{6}$$

where $\emptyset$ is the null set, let the l^{th} partition of the game is $\xi_l \in \Xi,\ 1 \leq l \leq O$, in this O is total number of partitions and Ξ is the set of all possible partitions. The utility i.e., data rate of the n^{th} user in the C_i coalition and ξ_l partition is denoted as $a_n(C_i, \xi_l)$. Assume coalition C_i has two users, $u_1, u_2 \in C_i$ and their channel coefficients satisfy the condition $|h_1|^2 < |h_2|^2$, $|C_i| \geq 2$, $C_i \subseteq N$. The utility or payoff of the k^{th} user with weak channel condition in coalition C_i is expressed as

$$a_k(C_i, \xi_l) = \log(1 + \frac{(\eta P_{\text{LED}}|g_{m,k}|)^2 P_{m,k}}{I_{\text{ICI}} + I_{\text{PICI}} + \overline{\sigma}^2_{m,k}}), \tag{7}$$

where I_{ICI} is the intra-cluster interference, I_{PICI} is the partial overlapping inter-cluster interference, and $\overline{\sigma}^2_{m,k}$ is the effective noise variance and it is explained in section III-A. Similarly, the utility of the K^{th} user with strong channel condition in coalition C_i is given by

$$a_K(C_i, \xi_l) = \log(1 + \frac{(\eta P_{\text{LED}}|g_{m,K}|)^2 P_{m,K}}{I_{\text{PICI}} + \overline{\sigma}^2_{m,K}}), \tag{8}$$

Then, the sum payoff of the coalition C_i and partition ξ_l is determined as

$$A(C_i, \xi_l) = \sum_{n \in C_i} a_n(C_i, \xi_l),\ \forall n \in C_i,\ 1 \leq i \leq M, \tag{9}$$

Coalition game-based user clustering in downlink NOMA is a cooperative game with non-transferable utility (NTU). Hence, it is necessary to convert the game from NTU into a transferable utility (TU) to facilitate user clustering. In this direction, the Shapley value calculation is applied to assign the payoff to each user with respect to coalitions. Therefore, the payoff i.e., Shapley value of the n^{th} user in coalition C_i and partition ξ_l can be written as

$$b_n(C_i, \xi_l) = \underbrace{\sum_{c_k \subseteq C_i \backslash n} \frac{|c_k|!(|C_i| - |c_k| - 1)!}{|C_i|!}}_{I} \times \underbrace{[A(c_k \cup \{n\}, \xi_l) - A(c_k, \xi_l)]}_{II}, \tag{10}$$

where c_k is the subset of C_i, i.e., $c_k \subseteq C_i,\ 1 \leq k \leq Q$, in this Q is the total number of subsets and the first term in (10) expresses the probability of the n^{th} user contribution and the second term is the n^{th} user marginal contribution. Using Shapley value, the sum payoff of the coalition C_i and partition ξ_l is computed as

$$B(C_i, \xi_l) = \sum_{n \in C_i} b_n(C_i, \xi_l),\ \forall n \in C_i,\ 1 \leq i \leq M, \tag{11}$$

D. PREFERENCE RELATION ALGORITHM (PRA)- TYPE I CLUSTERING

In this algorithm, each user checks their contribution while joining the new coalition; if the coalition value increases, then the user leaves the current coalition and joins the new coalition; otherwise, the user stays in the same coalition. Consider the two partitions ξ_1 and $\xi_2 \in \Xi$ and assume coalition C_i present in both partition. In this situation, the preference of the user is decided using the relation given below

$$(C_i, \xi_1) \preceq_n (C_i, \xi_2), \tag{12}$$

Algorithm 1 Preference Relation Algorithm- Type I

Initial state
Game start from the initial partition
$\xi_{ini} = \{C_1, C_2, \ldots, C_M\}$
Repeat
for *player* $n \in N$ *where* $n \in C_i$ **do**
  for *target coalition* $m \in M$ **do**
    if $m \neq n$ **then**
      if $(C_n, \xi_{cur}) \prec_n (C_m, \xi_{nxt})$ **then**
        $\{C_n, C_m\} = \{C_n \backslash \{n\}, C_m \cup \{n\}\}$;
        $\xi_{cur} = \xi_{nxt}$;
      end
    end
  end
end
Final state

where the notation $\preceq_n$ denote the preference of the n^{th} user. In the above expression (12), if the condition is satisfied then n^{th} user will move to partition ξ_2. Alternatively, the user's preference is decided within the same partition with different coalitions. Let C_1 and C_2 are the two clusters, then the condition for user preference is given by

$$(C_1, \xi_l) \preceq_n (C_2, \xi_l), \tag{13}$$

In PRA, the user coalition is initiated from the weak user, and it is selected by arranging the users in ascending order. Assume n^{th} user as a weak user want to join into m^{th} target coalition. Before joining the new coalition, the n^{th} user compares the sum rate with the current coalition and the m^{th} coalition using strict PRA. If the sum rate is improved, then the n^{th} user leaves the current coalition and joins into the m^{th} target coalition otherwise, the n^{th} user stays in the current coalition and then restart the joining process with the next target coalition and this process is continued until checking with all target coalitions. The second step in PRA is that if the n^{th} user is moved successfully into the target coalition or else cannot be moved anywhere, then the n^{th} user stops its process and then the next user will start the coalition process. This operation is repeated until checking with the last user. Now, the new partition structure is formed after one cycle of operation. Then, again the coalition process started with a new partition structure and repeated. If the users are not allowed to move into any target coalitions, then the process is stopped and the current partition structure will be considered as the desired partition. The procedures of PRA type-I are given in the algorithm.1

Using the above theory, the n^{th} user decides its coalition to improve the sum rate, thus the strict preference relation of the n^{th} user is expressed as

$$(C_i, \xi_1) \prec_n (C_i, \xi_2) \Leftrightarrow \sum_{i=1}^{M} B(C_i, \xi_1) < \sum_{i=1}^{M} B(C_i, \xi_2), \quad (14)$$

E. PRA- TYPE II CLUSTERING

Type II is similar to type I, except in type II the sum payoff is calculated without considering the partition. Thus, in type II the sum payoff improvement is achieved by simply swapping users between clusters, and user preference is decided by comparing the sum payoff of all users of those swapped clusters. Mathematical expression for the preference of the n^{th} user is given by

$$C_i \prec_n C_j \Leftrightarrow B(C_i) + B(C_j) < B(C_i \backslash \{n\}) + B(C_j \cup \{n\}), \quad (15)$$

where $B(C_i) = \sum_{n \in C_i} b_n(C_i)$, $\forall n \in C_i$, $1 \leq i \leq M$ is sum payoff of all users in cluster C_i which is similar to (11) except including the partition parameter ξ_l. PRA type II procedures is given in algorithm 2.

Algorithm 2 Preference Relation Algorithm-Type II

```
Initial state
The game start from the initial partition Repeat
for player n ∈ N where n ∈ C_i do
    for target coalition m ∈ M do
        if m ≠ n then
            if (C_n) ≺_n (C_m) then
                {C_n, C_m} = {C_n\{n}, C_m ∪ {n}};
            end
        end
    end
end
Final state
```

F. SEQUENCE GAME-BASED CLUSTERING

This algorithm is similar to the PRA type-I except in this game, only residual users play a game while a new coalition is leaving the game. Thus, the complexity of this game is less when compared to the PRA. Let the initial partition $\xi_{ini} = \{C_1, C_2, \ldots, C_M\}$ and assume one of the users start the game and leave from the current coalition and form a new coalition. Note that this user is allowed to form a new coalition only after all other users in this game can accept this proposal otherwise user can return to the current coalition. After this game, a new coalition is formed and then it leaves the game. Then, the game can be started with residual users and this process is continued until all the users joined into the new coalition. Finally, a new partition structure is formed which reaches the Nash equilibrium stable state.

Let us consider the current partition structure as given by

$$\xi_{cur} = \xi_{cur} \cup C_0, \text{ where } C_0 = \emptyset,$$

When the user starts the proposal in this sequencing game then a new partition is formed and it is expressed as

$$\xi_{nxt} = \{\xi_{cur} \backslash C_0, C_n\} \cup \{C_n \backslash \{n\}, C_0 \cup \{n\}\},$$

The detailed procedure of the sequence game is given in algorithm 3.

Algorithm 3 Sequence Game Based Algorithm

```
Initial state
Game start
players {1, 2, ... N} and n,m ∈ N
Initial partition ξ_ini = {C_1, C_2, ..., C_M}
Repeat
for player n ∈ N where n ∈ C_n do
    ξ_cur=ξ_cur ∪ C_0, where C_0 = ∅
    ξ_nxt = {ξ_cur\C_0, C_n} ∪ {C_n\{n}, C_0 ∪ {n}}
    Repeat
    if (C_n, ξ_cur) ≺_n (C_n, ξ_nxt) then
        ξ_cur = ξ_nxt
        for responder m ∈ N where m ∈ C_m do
            if m ≠ n then
                ξ_nxt =
                  {ξ_cur\C_0, C_m} ∪ {C_m\{m}, C_0 ∪ {m}}
                if (C_m, ξ_cur) ≺_m (C_m, ξ_nxt) then
                    ξ_cur = ξ_nxt
                end
            end
        end
    end
    ξ_cur = ξ_cur\{C_0}
end
Final state
```

G. STABILITY AND COMPLEXITY ANALYSIS

1) STABILITY ANALYSIS

In the preference relation type -1 algorithm, the user migration from one coalition to the other is decided by the strict preference condition which always increases the sum rate of the proposed network. Further, the sum rate due to the movement of the user is calculated by considering all the user's in the structure instead of users only in the specific coalitions. Also, in this case, the user follows the compare-and-swap operation and the final partitions are formed with the finite set. This final partition is converged into Nash-equilibrium stable state.

Similarly in the preference relation type-II algorithm, the user's migration between the coalitions is performed by compare-and-swap operation and the sum rate is calculated by considering only user's in the specific coalitions. Therefore, in this case, when the user moves to the new coalition the payoff of the users in the particular group only contributes to the improvement in the sum rate.

In sequence game algorithm, players move to the new coalition and the partition structure changed. Then, the game continues with residual players and the final partition is not always Nash's stable state. If the final partition is not Nash stable, then the player from the previous coalition starts the proposal and tries to form the final partition which satisfies the Nash stable state.

2) COMPLEXITY ANALYSIS

The computational complexity of the preference relation algorithm is based on how many times the compare-and-swap operations are performed by the users to reach the final partitions. Each user needs (N-1) time compare-and-swap operation therefore total N(N-1) times compare-and-swap operations are required for N users.

In sequence relation operation, the complexity is less due to limited compare-and-swap operation by the users because in this algorithm once the new coalition is formed it can leave the game, and swap operation is required only for the residual users. Each user needs (N-1) times compare-and-swap operation however, the total number of compare-and-swap operations is less than N(N-1).

III. PERFORMANCE ANALYSIS: D-OMA-VLC NETWORK

This section analyzes performance metrics of the proposed D-OMA VLC network, such as achievable rates, BER, and outage probability.

A. ACHIEVABLE RATES

Let us assume that the continuous data symbol is fed into the power amplifier which is denoted by $s_{m,k}$ with $\mathbb{E}\{s_{m,k}\} = 0$, variance $\mathbb{E}\{|s_{m,k}|^2\} = \varepsilon_{m,k}$, $-A < \varepsilon_{m,k} < A$ where A is the peak amplitude. After removing the DC bias, the received signal at $U_{m,k}$ can be expressed as in (16), shown at the bottom of the page, and η is the photo-detector responsivity in A/W, $g_{m,k}$ is the LoS VLC channel gain and $\omega_{m,k} \sim \mathcal{CN}(0, \sigma^2_{m,k})$ is the variance of additive white Gaussian noise (AWGN) at $U_{m,k}$ which is a combination of thermal and shot noise. The variance $\sigma^2_{m,k}$ of the noise can be expressed as

$$\sigma^2_{m,k} = \sigma^2_{shot} + \sigma^2_{ther}, \tag{17}$$

The shot noise in the optical communication can be modeled as

$$\sigma^2_{shot} = 2qB(\eta g_{m,k} s_{m,k} + I_{back} I_N), \tag{18}$$

where q is the electronic charge, I_{back} is the background current and I_N is the noise bandwidth factor. Similarly, the variance of the thermal noise in the VLC network can be expressed as [2]

$$\sigma^2_{ther} = \frac{8\pi K T_k}{G} C A I_N B^2 + \frac{16\pi^2 K T_k \Gamma}{g_m} C^2 A^2 I_3 B^3, \tag{19}$$

where K is the Boltzmann's constant, T_k is the absolute temperature, G is the open-loop voltage gain, C is the fixed capacitance of the PD per unit area, Γ is the field-effect transistor (FET) channel noise factor, g_m is the FET trans conductance and $I_3 = 0.0868$ [2]. The signal-to-interference plus noise ratio (SINR) for decoding its own messages at $U_{m,k}$ can be given as

$$\gamma_{m,k} = \begin{cases} \dfrac{(\eta P_{\text{LED}}|g_{m,k}|)^2 P_{m,k}}{I_{\text{ICI}} + I_{\text{PICI}} + \overline{\sigma}^2_{m,k}}, & k = 1, \ldots, K_m - 1, \\[2ex] \dfrac{(\eta P_{\text{LED}}|g_{m,k}|)^2 P_{m,k}}{I_{\text{PICI}} + \overline{\sigma}^2_{m,k}}, & k = K_m, \end{cases} \tag{20}$$

where $\overline{\sigma}_{m,k}$ is the effective variance of AWGN due to the expansion of bandwidth of the sub-band, i.e. $\overline{\sigma}_{m,k} = \sigma_{m,k}(1+ \delta^l_m + \delta^r_m)$. Also, the interference due to the signal of users in the same cluster is called intra-cluster interference (ICI), and the interference due to the signal of users in neighbor clusters is called as I_{PICI} are expressed as

$$I_{\text{ICI}} = \sum_{j=k+1}^{K_m} (\eta P_{\text{LED}}|g_{m,k}|)^2 P_{m,j}, \tag{21}$$

$$\begin{aligned} y_{m,k} = \eta P_{\text{LED}} \Bigg[& \underbrace{\sum_{i=1}^{k-1} g_{m,i}\sqrt{P_{m,i}} s_{m,i}}_{\text{SIC residual error}} + \underbrace{g_{m,k}\sqrt{P_{m,k}} s_{m,k}}_{\text{Desired signal}} + \underbrace{\sum_{j=k+1}^{K_m} g_{m,j}\sqrt{P_{m,j}} s_{m,j}}_{\text{ICI}} \\ & + \underbrace{\sum_{t=1}^{K_{m-1}} \left(\sqrt{\delta^l_m} + \sqrt{\delta^r_{m-1}}\right) g_{m,t}\sqrt{P_{m-1,t}} s_{m-1,t} + \sum_{y=1}^{K_{m+1}} \left(\sqrt{\delta^r_m} + \sqrt{\delta^l_{m+1}}\right) g_{m,y}\sqrt{P_{m+1,y}} s_{m+1,y}}_{\text{Partial ICI}} \Bigg] \\ & + \left(\sqrt{1 + \delta^l_m + \delta^r_m}\right) \omega_{m,k} \end{aligned} \tag{16}$$

and

$$I_{\text{PICI}} = (\eta P_{\text{LED}}|g_{m,k}|)^2 \left[\sum_{t=1}^{K_{m-1}} \left(\sqrt{\delta_m^l} + \sqrt{\delta_{m-1}^r}\right)^2 P_{m-1,t} + \sum_{y=1}^{K_{m+1}} \left(\sqrt{\delta_m^r} + \sqrt{\delta_{m+1}^l}\right)^2 P_{m+1,y} \right], \quad (22)$$

Finally, the achievable rates of the users belong to the attocell of BS is obtained through the lower bound of the capacity and it can be expressed as

$$R_{m,k} = \frac{B_m}{2} \log_2 \left(1 + \frac{e}{2\pi} \gamma_{m,k}\right), \quad k = 1, \ldots, K_m, \quad (23)$$

B. BIT ERROR RATES

In this sub-section, the bit error rate (BER) expressions of the proposed D-OMA-based VLC networks are derived using uni-polar OOK modulation. As in Fig. 2, a network with M clusters is considered and each cluster consists of K_m users. By applying maximum likelihood (ML) decoding, the m^{th} cluster k^{th} user $U_{\text{m,k}}$ can decode its message in the presence of the interferences. Mathematically, it can be written as

$$\hat{s}_{m,k} = \arg \min_x |y_{m,k} - \eta P_{\text{LED}} g_{m,k} \sqrt{P_{m,k}}|^2, \quad (24)$$

Assume that m^{th} cluster k^{th} user, $U_{m,k}$ decoded previous user's messages successfully i.e., $s_{m,1}, \ldots, s_{m,k-1}$, thus SIC error is omitted.[1] The conditional error probability of the m^{th} cluster k^{th} user, $U_{m,k}$ when the transmitted OOK symbol $s_{m,k} = 0$ is written as

$$p_{e|s_{m,k}=0} = \int_{\frac{P_s}{2}}^{\infty} \mathcal{N}(I_{\text{ICI}} + I_{\text{PICI}}, \sigma_{m,k})\, dy_{m,k}, \quad (25)$$

where $P_s = (\eta P_{\text{LED}}|g_{m,k}|)^2 P_{m,k}$ is the estimated desired signal power, $\mathcal{N}(\mu, \sigma_{m,k})$ denote the mean and variance of the Gaussian random variable $y_{m,k}$. After integrating the probability density function (PDF) of $y_{m,k}$, the error probability of the m^{th} cluster k^{th} user, $U_{m,k}$ can be expressed as [23]

$$p_{e|s_{m,k}=0} = \mathcal{Q}\left(\frac{1}{\sigma_{m,k}}\left(\frac{P_s}{2} - I_{\text{ICI}} - I_{\text{PICI}}\right)\right), \quad (26)$$

Similarly, the conditional error probability of the k^{th} user, $U_{m,k}$ when the transmitted OOK symbol $s_{m,k} = 1$ is given by

$$p_{e|s_{m,k}=1} = \int_{-\infty}^{\frac{P_s}{2}} \mathcal{N}(P_s + I_{\text{ICI}} + I_{\text{PICI}}, \sigma_{m,k})\, dy_{m,k}, \quad (27)$$

After some mathematical manipulations, the conditional error probability becomes

$$p_{e|s_{m,k}=1} = 1 - \mathcal{Q}\left(\frac{1}{\sigma_{m,k}}\left(-\frac{P_s}{2} - I_{\text{ICI}} - I_{\text{PICI}}\right)\right), \quad (28)$$

[1] Practically, SIC error occurs while decoding NOMA signal and it is modeled as a SIC residual error.

Using the identity $1 - \mathcal{Q}(x) = \mathcal{Q}(-x)$, the conditional error probability of m^{th} cluster and k^{th} user, $U_{m,k}$ can be further simplified as

$$p_{e|s_{m,k}=1} = \mathcal{Q}\left(\frac{1}{\sigma_{m,k}}\left(\frac{P_s}{2} + I_{\text{ICI}} + I_{\text{PICI}}\right)\right), \quad (29)$$

Proposition 1: In the proposed D-OMA scheme, the desired signal is affected by ICI and PICI thereby the effect of interference is more when compared to the massive in-band NOMA scheme where ICI only present. However, it is noteworthy that while reducing the cluster size in the D-OMA scheme the effect of ICI is significantly reduced and thus D-OMA scheme achieves similar performance to massive in-band NOMA. For example, consider six users with two clusters then massive in-band NOMA allows three users in each cluster and ICI comes from the two users in each cluster. At the same time, in the D-OMA scheme due to partially overlapping one more cluster is formed within the allocated bandwidth, therefore, two users are allocated to each cluster thus ICI comes from only one user in each cluster.

C. OUTAGE PROBABILITY

For the VLC downlink communication, if the user $U_{m,k}, k = 1, \ldots, K_m$ is failed to decode the signals of user $U_{m,i}, i = k, \ldots, K_m$, then the user communication is failed and tend to the outage. Let us assume the target data rate at $U_{m,k}$ is $\Re_{m,k}$ and then corresponding SINR can be written as $\Gamma_{m,k} = 2^{2\Re_{m,k}/B_m} - 1$. The outage probability of the user $U_{m,k}$ can be expressed as

$$P^o_{m,k} = 1 - \Pr\left\{ \cap_{i=1}^{k} \left(\gamma_{m,i} \geq \Gamma_{m,i}\right) \right\}, \quad (30)$$

By substituting from (20) into (30), we can further obtained the outage probability as

$$P^o_{m,k} = 1 - \Pr\left\{ \cap_{i=1}^{k} \left(|g_{m,i}|^2 \geq \epsilon_{m,i}\right) \right\}, \quad (31)$$

where

$$\epsilon_{m,i} = \begin{cases} \dfrac{\Gamma_{m,i}\left(I_{\text{PICI}} + \sigma^2_{m,i}\right)}{(\eta P_{\text{LED}})^2 [P_{m,k} - \Gamma_{m,i} \sum_{i=k+1}^{K_m} P_{m,i}]}, & i < K_m, \\ \dfrac{\Gamma_{iM_i}[I_{\text{PICI}} + \sigma_i^2]}{(\eta P_{\text{LED}})^2 [P_{m,k}}, & i = K_m, \end{cases} \quad (32)$$

As the users are distributed randomly and uniformly within the circular coverage area of the atto cell, the PDF of $r_{m,k}$ is given by $f_{r_{m,k}}(r_{m,k}) = 2r_{m,k}/r_0$. The PDF of $|g_{m,k}|^2$ is given as [34]

$$f_{|g_{m,k}|^2}(x) = \frac{\left[Z^{\mu+1}(\mu+1)C\right]^{\frac{2}{\mu+3}} x^{\frac{-\mu-4}{\mu+3}}}{r_0^2(\mu+3)}, \quad (33)$$

where boundaries of the variable x is given as

$$x_{min} = \frac{\left[Z^{\mu+1}(\mu+1)C\right]^2}{(r_0^2+z^2)^{\mu+3}}$$
$$x_{max} = \frac{\left[Z^{\mu+1}(\mu+1)C\right]^2}{z^{2(\mu+3)}}, \quad (34)$$

Let us take $\epsilon^*_{m,k} = \max\{\epsilon_{m,1}, \epsilon_{m,2}, \ldots, \epsilon_{m,k}\}$. The outage probability can be given as

$$P^o_{m,k} = \Pr\{|g_{m,k}|^2 > \epsilon^*_{m,k}\} = \int_{x_{min}}^{\epsilon^*_{m,k}} f_{|g_{m,k}|^2}(x)\, dx. \quad (35)$$

By considering two users cluster, a closed-form expression for the outage probability of the downlink VLC network can be obtained which is given in (40) and (41).

IV. D-OMA FOR VLC DOWNLINK COMMUNICATION

In downlink VLC networks, when the D-OMA scheme is employed, it can achieve better network performance when compared to the massive in-band NOMA. However, due to the overlapping of sub-bands, it can introduce the interference I_{PICI} which degrades the performance of the VLC network. Therefore, in order to reduce both I_{PICI} and I_{ICI} interference, we can design the D-OMA scheme with a smaller cluster size, preferably with two users clusters, so that the D-OMA scheme reduces the I_{PICI} interference. In this direction, all the N users are formed into a number of clusters, and each cluster consists of two users according to the game theory.

Hence the SINR of FU and NU of the m^{th} NOMA cluster, respectively, can be given as

$$\gamma_{m,f} = \frac{(\eta P_{\text{LED}}|g_{m,f}|)^2 P_{m,f}}{(\eta P_{\text{LED}}|g_{m,f}|)^2 P_{m,n} + I_{\text{PICI}_{m,f}} + \overline{\sigma}^2_{m,f}}, \quad (36)$$

and

$$\gamma_{m,n} = \frac{(\eta P_{\text{LED}}|g_{m,n}|)^2 P_{m,n}}{I_{\text{PICI}_{m,n}} + \overline{\sigma}^2_{m,n}}, \quad (37)$$

With two users clustering, the BER of the k^{th} user when the transmitted OOK symbol $s_{m,k} = 0$ can be expressed as

$$p_{e|s_{m,k}=0} = \mathcal{Q}\left(\frac{1}{\sigma_{m,k}}\left(\Omega_{m,f} - \Omega_{m,n} - I_{\text{PICI}}\right)\right), \quad (38)$$

where $\Omega_{m,f} = (\eta P_{\text{LED}}|g_{m,f}|)^2 P_{m,f}$ and $\Omega_{m,n} = (\eta P_{\text{LED}}|g_{m,f}|)^2 P_{m,n}$ are the desired signal and ICI. Similarly, the BER of the k^{th} user when the transmitted OOK symbol $s_{m,k} = 1$ is written as

$$p_{e|s_{m,k}=1} = \mathcal{Q}\left(\frac{1}{\sigma_{m,k}}\left(\Omega_{m,f} + \Omega_{m,n} + I_{\text{PICI}}\right)\right), \quad (39)$$

Similarly, the outage probability of the FU and NU in the m^{th} NOMA cluster, respectively, can be given as

$$P^o_{m,f} = \frac{\left[Z^{\mu+1}(\mu+1)C\right]^{\frac{2}{\mu+3}}}{r_0^2}\left(x_{min}^{\frac{-1}{\mu+3}} - \epsilon_{m,f}^{\frac{-1}{\mu+3}}\right), \quad (40)$$

and

$$P^o_{m,n} = \frac{\left[Z^{\mu+1}(\mu+1)C\right]^{\frac{2}{\mu+3}}}{r_0^2}\left(x_{min}^{\frac{-1}{\mu+3}} - \epsilon_{m,n}^{\frac{-1}{\mu+3}}\right), \quad (41)$$

where

$$\epsilon_{m,f} = \frac{\Gamma_{m,f}\left(I_{\text{PICI}} + \sigma^2_{m,f}\right)}{(\eta P_{\text{LED}})^2 P_{m,f} - \Gamma_{m,f} P_{m,f}]}, \quad (42)$$

and

$$\epsilon_{m,n} = \frac{\Gamma_{m,n}[I_{\text{PICI}} + \sigma^2_{m,n}]}{(\eta P_{\text{LED}})^2 P_{m,n}}, \quad (43)$$

V. TRANSMISSION POWER MINIMIZATION

In this Section, we minimize the total transmission power of a NOMA cluster, under the QoS requirements, outage constraints, and dimming control. In dimming control, the average optical power is controlled as per the illumination requirements of the environment. The average optical power $P_o^{avg} = I_{\text{DC}} = \tau P_T$, where τ is the dimming level and P_T is the maximum optical power. Also, to ensure eye safety, the maximum permissible current of the LED, I_H should be limited as $\sqrt{P_{m,k}}A + I_{\text{DC}} \leq I_H$. The optimization problem can be expressed as

$$\min_{P_{m,k}, I_{\text{DC}}} \quad \sum_{k=1}^{K_m} \varepsilon_{m,k}\, P_{m,k} + I_{\text{DC}}^2 \quad (44a)$$
$$\text{s.t.} \quad R_{m,k} \geq \Re_{m,k}, \quad \forall k = 1, \ldots, K_m, \quad (44b)$$
$$P^o_{m,k} \leq \varrho^o_{m,k}, \quad \forall k = 1, \ldots, K_m, \quad (44c)$$
$$\sqrt{P_{m,k}}A + I_{\text{DC}} \leq I_H, \quad \forall k = 1, \ldots, K_m, \quad (44d)$$
$$I_{\text{DC}} = \tau\, P_T, \quad (44e)$$
$$P_{m,k} \geq 0, \quad I_{\text{DC}} \geq 0, \quad (44f)$$

The outage probability constraint is also taken into the optimization problem and $\varrho^o_{m,k}$ is the outage probability limit for successful communication between $\text{U}_{m,k}$ and the BS. In the proposed D-OMA for VLC communication, users are grouped to have only two users in a NOMA cluster i.e. two user clustering. Hence the allocated power for the NU and FU, respectively, can be expressed as $\alpha_m P_N$ and $(1-\alpha_m)P_N$, where α_m is the power allocation coefficient of the m^{th} NOMA cluster and P_N is the maximum power allocated for a sub-band. Therefore, the optimization problem can be reformulated as

$$\min_{\alpha_m, I_{\mathrm{DC}}} \quad \varepsilon_{m,f}\ \alpha_m P_N + \varepsilon_{m,n}\ (1-\alpha_m)P_N + I_{\mathrm{DC}}^2 \tag{45a}$$

$$\text{s.t.} \quad R_{m,f} \geq \Re_{m,f}, \quad R_{m,n} \geq \Re_{m,n}, \tag{45b}$$

$$P_{m,f}^o \leq \varrho_{m,f}^o, \quad P_{m,n}^o \leq \varrho_{m,n}^o, \tag{45c}$$

$$\sqrt{P_N}A + I_{\mathrm{DC}} \leq I_H, \tag{45d}$$

$$I_{\mathrm{DC}} = \tau\ P_{\mathrm{LED}} I_H, \tag{45e}$$

$$\alpha_m \geq 0, \quad I_{\mathrm{DC}} \geq 0, \tag{45f}$$

Since the Hessian matrix of the objective function is positive and semi-definite, the optimization problem is convex under the considered constraints. Therefore, the Lagrange function of the above problem can be expressed as

$$\begin{aligned}\mathcal{L}(\alpha_m, I_{\mathrm{DC}}, \lambda_1, \lambda_2, \lambda_3, \lambda_4, \lambda_5, \lambda_6) &= P_t \\ &+\lambda_1(\Re_{m,f} - R_{m,f}) + \lambda_2(\Re_{m,n} - R_{m,n}) \\ &+\lambda_3(P_{m,f}^o - \varrho_{m,f}^o) + \lambda_4(P_{m,n}^o - \varrho_{m,n}^o) \\ &+\lambda_5(I_H - \sqrt{P_N}A + I_{\mathrm{DC}}) \\ &+\lambda_6(I_{\mathrm{DC}} - \tau\ P_{\mathrm{LED}} I_H),\end{aligned} \tag{46}$$

where $P_t = \varepsilon_{m,f}\ \alpha_m P_N + \varepsilon_{m,n}\ (1-\alpha_m)P_N + I_{\mathrm{DC}}^2$ is the total transmission power of the m^{th} NOMA cluster and $\lambda_i, i \in \{1,\ldots,6\}$ are the Lagrange multiplier. By taking the derivations of (44) and applying Karush-Kuhn Tucker (KKT) conditions, optimal solutions for α_m and I_{DC} can be obtained. Consequently, the derivatives of (44) with respect to α_m, I_{DC}, and λ_i, respectively, can be given as

$$\frac{\partial \mathcal{L}}{\partial \alpha_m} = (\varepsilon_{m,f} - \varepsilon_{m,n})P_N - \lambda_1 \frac{\partial R_{m,f}}{\partial \alpha_m} - \lambda_2 \frac{\partial R_{m,n}}{\partial \alpha_m} - \lambda_3 \frac{\partial P_{m,f}^o}{\partial \alpha_m} - \lambda_4 \frac{\partial P_{m,n}^o}{\partial \alpha_m} \leq 0, \tag{47a}$$

$$\frac{\partial \mathcal{L}}{\partial I_{DC}} = 2I_{\mathrm{DC}} + \lambda_5 + \lambda_6 \leq 0, \tag{47b}$$

$$\frac{\partial \mathcal{L}}{\partial \lambda_1^*} = \Re_{m,f} - R_{m,f} \geq 0, \quad \frac{\partial \mathcal{L}}{\partial \lambda_2^*} = \Re_{m,n} - R_{m,n} \geq 0, \tag{47c}$$

$$\frac{\partial \mathcal{L}}{\partial \lambda_3^*} = P_{m,f}^o - \varrho_{m,f}^o \geq 0, \quad \frac{\partial \mathcal{L}}{\partial \lambda_4^*} = P_{m,n}^o - \varrho_{m,n}^o \geq 0, \tag{47d}$$

$$\frac{\partial \mathcal{L}}{\partial \lambda_5^*} = I_H - \sqrt{P_N}A + I_{\mathrm{DC}} \geq 0, \tag{47e}$$

$$\frac{\partial \mathcal{L}}{\partial \lambda_6^*} = I_{\mathrm{DC}} - \tau\ P_{\mathrm{LED}} I_H \geq 0, \tag{47f}$$

By applying KKT conditions, the optimal solutions of α_m and I_{DC}, respectively, can be obtained.

$$\alpha_m^* = \frac{\Pi_1^2\ \Delta\ X + \Pi_1^2\ \Delta^2\ X + \Pi_2}{\Pi_1^2\ \Delta\ X + \Pi_1 + \Pi_2}, \tag{48}$$

and

$$I_{\mathrm{DC}}^* = \frac{\tau P_{\mathrm{LED}} \sqrt{P_N}A}{1 + \tau P_{\mathrm{LED}}}, \tag{49}$$

TABLE 1. Simulation parameters.

S.No.	*Parameters*	*Symbol*	*Value*
1.	Distance between the NU and the BS	d_1	1 m, 2 m and 3 m
2.	Distance between the FU and the BS	d_2	4 m, 6 m and 8 m
3.	Path loss exponent	υ	2
4.	Optical detection area	A	0.01
5.	FOV	ϕ_c	60°
6.	LED semi-angle	$\phi_{1/2}$	40°, 60°
7.	Angle of irradiance	φ_1, φ_2	40°, 30°
8.	Angle of incidence	ϕ_1, ϕ_2	35°, 45°
9.	LED power	P_{LED}	20 W/A
10.	PD responsitivity	η	0.4 A/W
11.	Refractive index	ν	1.5
12.	Gain of the optical filter	$T(\phi_i)$	1

*BS - base station, NU - near user, FU - far user

where,

$$\begin{aligned}\Pi_1 &= (\eta P_{LED}|g_{m,f}|)^2 P_N, \\ \Pi_2 &= (\eta P_{LED}|g_{m,n}|)^2 P_N, \\ \Delta &= \left(\sqrt{\delta_m^l} + \sqrt{\delta_{m-1}^r}\right)^2 + \left(\sqrt{\delta_m^r} + \sqrt{\delta_{m+1}^l}\right)^2, \\ X &= 2^{\frac{2\Re_{m,f}}{B_m}} - 2^{\frac{2\Re_{m,n}}{B_m}},\end{aligned} \tag{50}$$

VI. RESULTS AND DISCUSSION

In this section, the sum rate, BER, and outage probability of the proposed D-OMA-VLC network are analyzed. In all the simulations, the VLC downlink channel is used as a DC channel and OOK modulation is considered. The proposed D-OMA VLC network is compared with massive in-band NOMA. The simulation parameters are listed in the Table. 1.

The sum-rate performance of the proposed D-OMA-VLC network is shown in Fig. 3. In this simulation, four users are considered for the clustering. In PRA, users are not classified as near and far users and grouping is formed using Shapley value calculation. In random NOMA, grouping is performed using near-user and far-user channel conditions. Further, two sets of distances are considered to analyze the sum-rate variation due to distances. It is noted that the sum rate of the proposed D-OMA-VLC network is significantly improved compared to the random NOMA because each user's payoff depends on the users' coalition. However, the sum rate of the random NOMA is better than the existing OMA scheme. Also, it is observed that the sum rate of the network using the clustering algorithm is improved with respect to the distance. Particularly, the sum-rate improvement is achieved when the distance is decreased.

Sum-rate performance of the proposed D-OMA-VLC network using type-I PRA is compared with type-II PRA in Fig. 4. Shapley value calculation is employed in both type-I and type-II PRA methods. It is noted that type-I PRA achieves a better sum rate when compared to the type-II PRA because, in the type-I coalition, user preference is decided along with their type of partition. Therefore, coalition value is improved

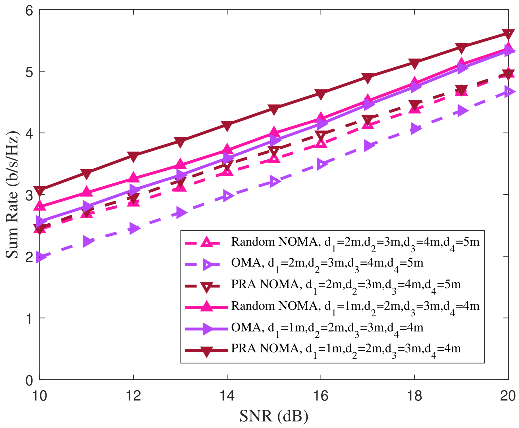

FIGURE 3. Sum-rate performance of the proposed D-OMA VLC network using clustering algorithm.

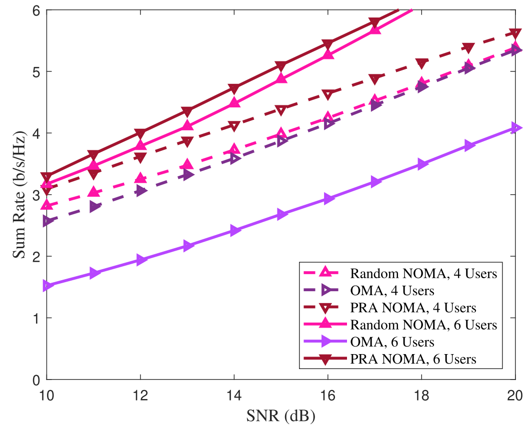

FIGURE 5. Sum-rate performance of the proposed D-OMA VLC network using different users.

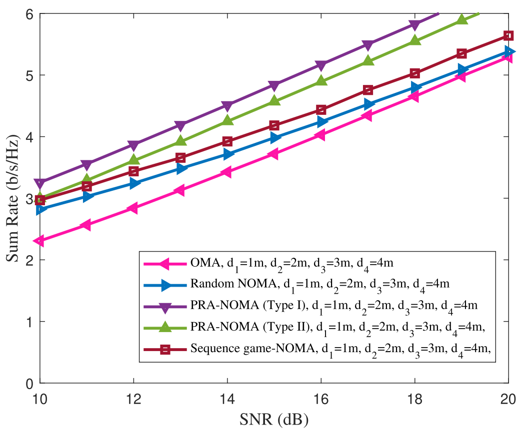

FIGURE 4. Comparison of the sum-rate performance of the proposed D-OMA VLC network.

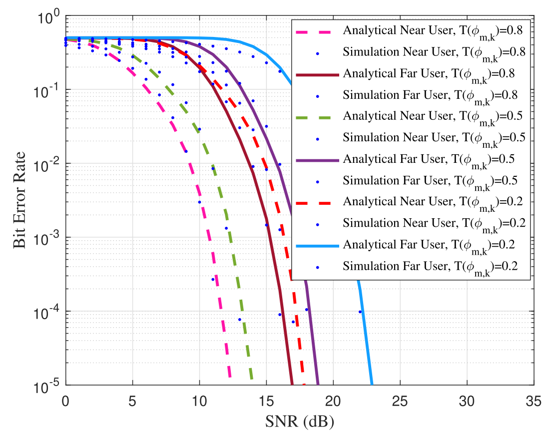

FIGURE 6. BER performance of the proposed D-OMA VLC network under various $T(\phi_{m,k})$ values.

when compared to the users swapping among the clusters without considering the type of partitions.

Fig. 5 shows the sum-rate performance of the proposed D-OMA VLC network with different users. In this simulation, clustering is formed using four users and six users. All the simulation setup are considered as in the previous figure. It is noted that the improvement in the users clustering is achieved when the number of users is increased within the cluster. Also, it is noted that user clustering does not improve the performance of the network while operating with the OMA scheme.

BER performance of the proposed D-OMA VLC network is shown in Fig. 6. The following simulation parameters are considered: the I_{ICI} power is 0 dB, I_{PICI} power is -10 dB [32], the distance of the near user taken as 2 m and far user is 4 m. Simulation results are plotted to validate the analytical results. It is observed that when increasing the optical filter gain, the BER performance of the downlink D-OMA VLC network is significantly improved. Therefore, the optical filter gain is identified as one of the main factors in improving the performance of the VLC networks.

Fig. 7 shows the BER performance of the downlink D-OMA VLC network. Distances of near and far users are taken as in the attocell dimensions. In this simulation, the I_{ICI} power is considered as 0 dB and I_{PICI} power is -10 dB. The distances of the far users are considered as 2 m, 4 m, and 6 m. It is observed that the proposed D-OMA user with the distance of 2 m achieves around 5 dB SNR gain when compared with massive in-band NOMA-VLC networks. Also, it is noted that even with increasing the distance, D-OMA far users still maintain a good SNR gain due to the smaller cluster size.

The BER performance of the proposed D-OMA-VLC network is shown in Fig. 8. In this simulation, two clusters are considered and each cluster consists of one near the user and one far user [33]. The distances of the near user and far user of the first cluster are 1 m and 2 m respectively. Similarly, the distance of the users in the second cluster is 3 m and 6 m. The sub-band overlapping interference $I_{\text{PICI}} = -10$ dB. It is noteworthy that the BER performance of cluster 1 is better than cluster 2. This is because the distances of the users in cluster 1 are small when compared to cluster 2. Also, it is

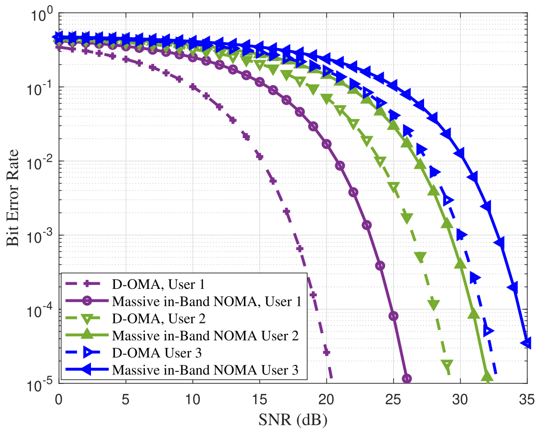

FIGURE 7. Comparison of BER performance with various multiple access techniques.

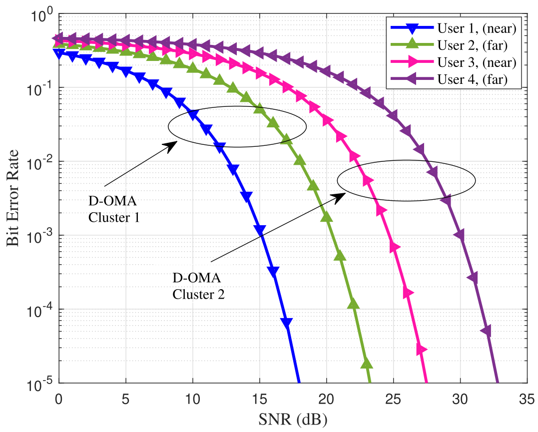

FIGURE 8. BER performance of the D-OMA-VLC with two users cluster size.

noted that the cluster near the user has better BER results than the far user. Further, it is interesting to note that even though the proposed D-OMA-VLC network operates with small cluster sizes, it maintains a similar performance to the massive in-band NOMA. Fig. 9 shows the BER performance of the proposed D-OMA-VLC for different FOV. The values of sub-band overlapping parameter δ are 0.01 and 0.001. Two user cluster is considered with the distance of 2 m and 4 m. FOV of LED light varied from 40° to 90°. Assumed LOS path between the users and LED. It is noted that when the degree of angle of FOV increases, the BER of the user within the cluster gradually increases. Thus, it gives the idea about the choice of FOV value to get better performance of the VLC wireless network.

The BER performance of the proposed D-OMA-VLC network is shown in Fig. 10 for various values of the photodetector areas, A. In this simulation, FOV values are considered as 40°, 45° and 50° and the sub-band overlapping interference $I_{\text{PICI}} = -10$ dB. It is observed that the BER of the proposed network is decreased when increasing the photodetector area. Also, the impact of the photodetector area on optical light

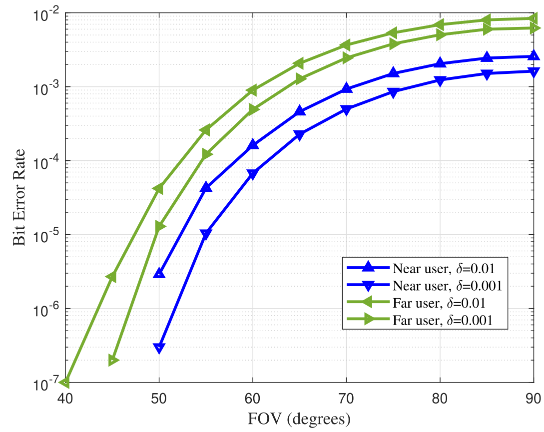

FIGURE 9. BER performance of the D-OMA VLC network for different FOV.

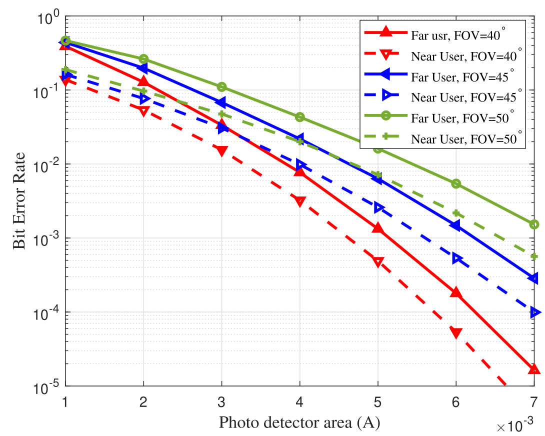

FIGURE 10. BER performance of the D-OMA VLC network with different photo detector areas and I_{PICI}=-10dB.

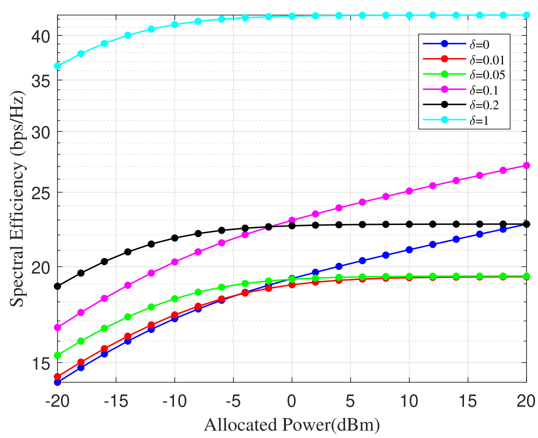

FIGURE 11. Comparison of spectral efficiency versus allocated power for different δ values.

communication is evident. At $A = 5 \times 10^{-3}$, the BER of the far user is 10^{-2} with FOV of 50° whereas 10^{-3} for FOV of 40°.

The spectral efficiency of the proposed D-OMA-VLC network is shown in Fig. 11. For D-OMA, the left side and

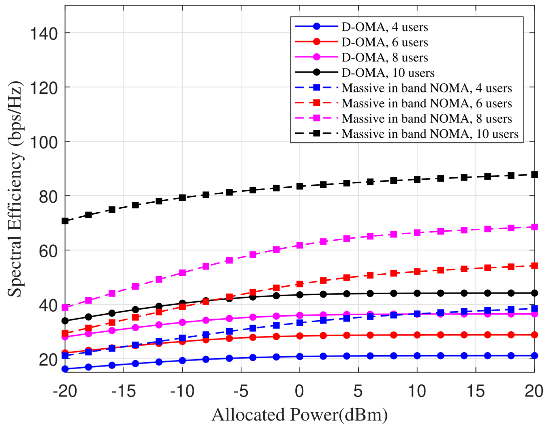

FIGURE 12. Comparison of spectral efficiency versus allocated power for a different number of users.

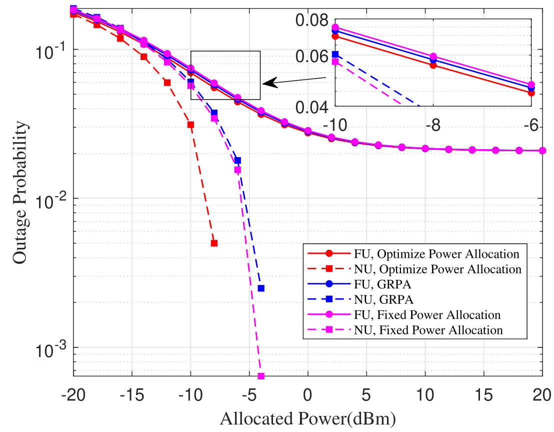

FIGURE 13. Comparison of outage Probability versus allocated power for different power allocation schemes.

TABLE 2. List of symbols.

Symbol	Parameter
α_m	power allocation coefficient
$\Phi_{m,k}$	field of view (FoV)
$\phi_{m,k}$	angle of incidence
$\varphi_{m,k}$	angle of irradiation
μ	order of Lambertian emission
$\varphi_{1/2}$	LED semi-angle
ν	refractive index
$\emptyset$	null set
$\sigma^2_{m,k}$	noise variance
$\mathcal{Q}(.)$	Q-function

right side sub-band overlapping coefficient is taken as δ. Sub-band overlapping coefficient δ varied from 0 to 0.2 in this simulation. At $\delta = 0$, the proposed network match with a massive in-band NOMA-VLC network. The figure clearly shows the effect of the sub-band overlapping in the proposed D-OMA-VLC network at a high SNR regime. Also, it is noteworthy that the spectral efficiency achieves its highest values at $\delta = 1$. However, increasing the δ results in the highest partial ICI. At $\delta = 0.1$, D-OMA provides better spectral efficiency for the considered allocated power levels. Moreover, it is noted that at the value of $\delta = 0.1$, the network achieves the reasonable spectral efficiency of 20 $b/s/Hz$. Thus, the proposed network guarantees the network capacity with allowed sub-band overlapping.

Fig. 12 shows the comparison of the spectral efficiency of the proposed D-OMA-VLC with a massive in-band NOMA-VLC network. For D-OMA, sub-band overlapping percentage δ is set to 0.1. Clusters with four users, six users, eight users, and ten users are considered for massive in-band NOMA. In the proposed D-OMA, four users cluster is split into two users clusters. Similarly, six users, eight users, and ten users clusters are split into a number of two user clusters. Hence, the spectral efficiency of the proposed D-OMA-VLC network is less when compared with the massive in-band NOMA-VLC network, even though it achieves better reliability and massive connectivity.

TABLE 3. List of acronyms.

Acronym	Full form
5G	fifth generation
6G	sixth generation
AWGN	additive white Gaussion noise
BER	bit error rate
BPSK	binary phase shift keying
BS	base station
CSI	channel state information
DC	direct current
D-OMA	delta- orthogonal multiple access
FET	field effect transistor
FFT	fast Fourier transform
FU	far user
GRPA	gain ratio power allocation
IM/DD	intensity modulation/direct detection
IoT	internet of things
KKT	Karush-Kuhn Tucker
MA	multiple access
mMTC	massive machine type communication
MMSE	minimum mean square error
NOMA	non orthogonal multiple access
NU	near user
NTU	non-transferable utility
OFDMA	orthogonal frequency division multiple access
OOK	on-off keying
OWC	optical wireless communication
PAPR	peak average power ratio
PICI	partial overlapping inter-cluster interference
PRA	preference relation algorithm
SIC	successive interference cancellation
SINR	signal to interference plus noise ratio
SNR	signal to noise ratio
TU	transferable utility
uHDD	ultra-high data density
uHSLLC	ultra-high-speed with low-latency communications
uMUB	ubiquitous mobile ultra-broadband
VL	visible light

The outage probability of the NU and FU of the proposed D-OMA-VLC network for different power allocation schemes is shown in Fig. 13. The optimized values of α and

I_{DC} are used to obtain the simulation results. The performance of optimized power allocation is compared with the existing gain ratio power allocation (GRPA) and fixed power allocation. The sub-band overlapping percentage δ is set to 0.1, and the QoS requirement for both NU and FU is set to 0.5 bps/Hz. For optimized power allocation, the outage probability of both NU and FU shows better performance than the GRPA and fixed power allocation. NU performs better outage in all power allocation schemes, especially at a low SNR regime. On the other hand, the performance of the FU is limited due to ICI and PICI at allocated power values. Although the allocated power increases, the outage performance of the FU remains at a fixed value at high allocated power values.

VII. CONCLUSION

A new multiple access schemes D-OMA enabled VLC network model is proposed to enhance the accessibility and rate of indoor wireless networks. The performance of the proposed D-OMA-VLC network is compared with the massive in-band NOMA-VLC network in terms of spectral efficiency, BER, and outage probability. Numerical results conclude that the sum rate of the proposed D-OMA-based VLC network outperforms the existing in-band NOMA scheme. Further, power optimization is performed at the downlink transmission of the proposed network, which ensures the QoS of the users within the clusters of the network. Therefore, the proposed VLC model will support many indoor applications with a high rate and large access.

REFERENCES

[1] M. Z. Chowdhury, M. T. Hossan, A. Islam, and Y. M. Jang, "A comparative survey of optical wireless technologies: Architectures and applications," *IEEE Access*, vol. 6, pp. 9819–9840, 2018.

[2] T. Komine and M. Nakagawa, "Fundamental analysis for visible-light communication system using LED lights," *IEEE Trans. Consum. Electron.*, vol. 50, no. 1, pp. 100–107, Feb. 2004.

[3] P. H. Pathak, X. Feng, P. Hu, and P. Mohapatra, "Visible light communication, networking, and sensing: A survey, potential and challenges," *IEEE Commun. Surveys Tuts.*, vol. 17, no. 4, pp. 2047–2077, 4th. Quart., 2015.

[4] A. Jabban, S. Haese, and M. Helard, "Theoretical and experimental optimization of DMT-based visible light communication under lighting constraints," *EURASIP J. Wireless Commun. Netw.*, vol. 2020, no. 1, pp. 1–29, Dec. 2020.

[5] K. David and H. Berndt, "6G vision and requirements: Is there any need for beyond 5G?" *IEEE Veh. Technol. Mag.*, vol. 13, no. 3, pp. 72–80, Sep. 2018.

[6] A. Jovicic, J. Li, and T. Richardson, "Visible light communication: Opportunities, challenges and the path to market," *IEEE Commun. Mag.*, vol. 51, no. 12, pp. 26–32, Dec. 2013.

[7] H. Marshoud, V. M. Kapinas, G. K. Karagiannidis, and S. Muhaidat, "Non-orthogonal multiple access for visible light communications," *IEEE Photon. Technol. Lett.*, vol. 28, no. 1, pp. 51–54, Jan. 1, 2016.

[8] Y. Qiu, H.-H. Chen, and W.-X. Meng, "Channel modeling for visible light communications—A survey," *Wireless Commun. Mobile Comput.*, vol. 16, no. 14, pp. 2016–2034, Oct. 2016.

[9] R. C. Kizilirmak, C. R. Rowell, and M. Uysal, "Non-orthogonal multiple access (NOMA) for indoor visible light communications," in *Proc. 4th Int. Workshop Opt. Wireless Commun. (IWOW)*, Istanbul, Turkey, Sep. 2015, pp. 95–101.

[10] D. A. Wiegandt, C. R. Nassar, and Z. Wu, "Overcoming peak-to-average power ratio issues in OFDM via carrier-interferometry codes," in *Proc. IEEE 54th Veh. Technol. Conf. (VTC Fall)*, Atlantic City, NJ, USA, Oct. 2001, pp. 660–663.

[11] M. Kashef, M. Abdallah, and K. Qaraqe, "Power allocation for downlink multi-user SC-FDMA visible light communication systems," in *Proc. 49th Annu. Conf. Inf. Sci. Syst. (CISS)*, Baltimore, MD, USA, Mar. 2015, pp. 1–5.

[12] M. Hua, B. Ren, M. Wang, J. Zou, C. Yang, and T. Liu, "Performance analysis of OFDMA and SC-FDMA multiple access techniques for next generation wireless communications," in *Proc. IEEE 77th Veh. Technol. Conf. (VTC Spring)*, Dresden, Germany, Jun. 2013, pp. 1–4.

[13] H. S. Eshwaraiah and A. Chockalingam, "SC-FDMA for multiuser communication on the downlink," in *Proc. 5th Int. Conf. Commun. Syst. Netw. (COMSNETS)*, Bangalore, India, Jan. 2013, pp. 1–7.

[14] C. Ciochina and H. Sari, "A review of OFDMA and single-carrier FDMA and some recent results," *Adv. Electon. Telecommun.*, vol. 1, no. 1, pp. 35–40, Apr. 2010.

[15] Z. J. Ali, N. K. Noordin, A. Sali, and F. Hashim, "Fair energy-efficient resource allocation for downlink NOMA heterogeneous networks," *IEEE Access*, vol. 8, pp. 200129–200145, 2020.

[16] H. Y. Lee and S. Y. Shin, "A novel user grouping in phase rotation based downlink NOMA," *IEEE Access*, vol. 10, pp. 27211–27222, 2022.

[17] S. Rajkumar, D. N. K. Jayakody, and Z. Chang, "A hybrid NOMA-PLNC wireless relay scheme," in *Proc. IEEE 18th Annu. Consum. Commun. Netw. Conf. (CCNC)*, Las Vegas, NV, USA, Jan. 2021, pp. 1–2.

[18] S. Rajkumar and D. N. K. Jayakody, "Backscatter assisted NOMA-PLNC based wireless networks," *Sensors*, vol. 21, no. 22, p. 7589, Nov. 2021.

[19] J. Song, T. Cao, and H. Zhang, "A low complexity NOMA scheme in VLC systems using pulse modulations," in *Proc. 29th Wireless Opt. Commun. Conf. (WOCC)*, Newark, NJ, USA, May 2020, pp. 1–6.

[20] H. Peng, Q. Li, A. Pandharipande, X. Ge, and J. Zhang, "Performance analysis of a SLIPT-based hybrid VLC/RF system," in *Proc. IEEE/CIC Int. Conf. Commun. China (ICCC)*, Chongqing, China, Aug. 2020, pp. 360–365.

[21] S. Rajkumar and D. N. K. Jayakody, "Optimal power allocation in hybrid NOMA-PLNC network with ambient backscattering," in *Proc. 10th Int. Conf. Inf. Automat. Sustainability (ICIAfS)*, Negambo, Sri Lanka, Aug. 2021, pp. 25–30.

[22] Z. Tahira, H. M. Asif, A. A. Khan, S. Baig, S. Mumtaz, and S. Al-Rubaye, "Optimization of non-orthogonal multiple access based visible light communication systems," *IEEE Commun. Lett.*, vol. 23, no. 8, pp. 1365–1368, Aug. 2019.

[23] H. Marshoud, P. C. Sofotasios, S. Muhaidat, G. K. Karagiannidis, and B. S. Sharif, "Error performance of NOMA VLC systems," in *Proc. IEEE Int. Conf. Commun. (ICC)*, Paris, France, May 2017, pp. 1–6.

[24] X. Liu, Z. Chen, Y. Wang, F. Zhou, Y. Luo, and R. Q. Hu, "BER analysis of NOMA-enabled visible light communication systems with different modulations," *IEEE Trans. Veh. Technol.*, vol. 68, no. 11, pp. 10807–10821, Nov. 2019.

[25] E. M. Almohimmah and M. T. Alresheedi, "Error analysis of NOMA-based VLC systems with higher order modulation schemes," *IEEE Access*, vol. 8, pp. 2792–2803, 2019.

[26] W. Saad, Z. Han, M. Debbah, A. Hjørungnes, and T. Basar, "Coalitional game theory for communication networks," *IEEE Signal Process. Mag.*, vol. 26, no. 5, pp. 77–97, May 2009.

[27] K. Wang, Z. Ding, and W. Liang, "A game theory approach for user grouping in hybrid non-orthogonal multiple access systems," in *Proc. Int. Symp. Wireless Commun. Syst. (ISWCS)*, Poznan, Poland, Sep. 2016, pp. 643–647.

[28] M. S. Ali, H. Tabassum, and E. Hossain, "Dynamic user clustering and power allocation for uplink and downlink non-orthogonal multiple access (NOMA) systems," *IEEE Access*, vol. 4, pp. 6325–6343, 2016.

[29] Y. Liu, Z. Huang, W. Li, and Y. Ji, "Game theory-based mode cooperative selection mechanism for device-to-device visible light communication," *Opt. Eng.*, vol. 55, no. 3, Mar. 2016, Art. no. 030501.

[30] X. Zhang, Q. Gao, C. Gong, and Z. Xu, "User grouping and power allocation for NOMA visible light communication multi-cell networks," *IEEE Commun. Lett.*, vol. 21, no. 4, pp. 777–780, Apr. 2017.

[31] Y. Al-Eryani and E. Hossain, "The D-OMA method for massive multiple access in 6G: Performance, security, and challenges," *IEEE Veh. Technol. Mag.*, vol. 14, no. 3, pp. 92–99, Sep. 2019.

[32] M. Z. Chowdhury, M. Shahjalal, S. Ahmed, and Y. M. Jang, "6G wireless communication systems: Applications, requirements, technologies, challenges, and research directions," *IEEE Open J. Commun. Soc.*, vol. 1, pp. 957–975, 2020.

[33] E. Hossain and Y. Al-Eryani, ''Large-scale NOMA: Promises for massive machine-type communication,'' in *Proc. IEEE COMSOC TCCN Newslett.*, Charlottesville, VA, USA, Dec. 2018, pp. 1–5.

[34] L. Yin, W. O. Popoola, X. Wu, and H. Haas, ''Performance evaluation of non-orthogonal multiple access in visible light communication,'' *IEEE Trans. Commun.*, vol. 64, no. 12, pp. 5162–5175, Dec. 2016.

PRIYASHANTHA TENNAKOON (Member, IEEE) received the B.Sc. degree (Hons.) in electrical and information engineering from the University of Ruhuna, Matara, Sri Lanka, in 2013. He is currently pursuing the Ph.D. degree with Lusófona University, Lisbon, Portugal. From August 2013 to December 2017, he was a Research Assistant with the Department of Electronics and Telecommunication, University of Moratuwa, Moratuwa, Sri Lanka. He was a Research Associate with the School of Engineering, Sri Lanka Technological Campus, Padukka, Sri Lanka, from January 2018 to February 2020. He has been working as a Lecturer with the Department of Electrotechnology, Wayamba University of Sri Lanka, Sri Lanka. His research interests include stochastic wireless channel modeling, visible light communication (VLC), simultaneous light-wave information and power transfer (SLIPT), and non-orthogonal multiple access (NOMA).

SAMIKKANNU RAJKUMAR (Member, IEEE) received the B.E. degree in electronics and communication engineering from the Angala Amman College of Engineering and Technology, Tamil Nadu, India, in 2000, the M.E. degree in communication systems from the Thiagarajar College of Engineering, Tamil Nadu, in 2006, and the Ph.D. degree in wireless communication from Anna University, Chennai, India, in 2015. Currently, he is working as a Research Scientist with the Centre for Telecommunication Research, Sri Lanka Technological Campus, Padukka, Sri Lanka. He has published several refereed papers in various international journals and conferences. His current research interests include non-orthogonal multiple access technique, physical layer security, visible light communication, and soft information relay.

DUSHANTHA NALIN K. JAYAKODY (Senior Member, IEEE) received the M.Sc. degree in electronics and communications engineering from the Department of Electrical and Electronics Engineering, Eastern Mediterranean University, Turkey, under the university full graduate scholarship, and the Ph.D. degree in electronics and communications engineering from University College Dublin, Ireland, in 2014.

From 2014 to 2016, he was a Postdoctoral Research Fellow at the University of Tartu, Estonia, and the University of Bergen, Norway. He held a visiting and/or sabbatical positions at the Center for Telecommunications Research, The University of Sydney, Australia, in 2015, and Texas A&M University, in 2018. From 2016 to 2021, he was a Professor at the School of Computer Science and Robotics, National Research Tomsk Polytechnic University (TPU), Russia. He was a Visiting Professor at the University of Jyvaskyla, Finland, in 2019 and 2022, with in the framework of the Academy of Finland. He also worked as a Visiting Professor at the University of Juiz de Fora, Brazil, in 2019. From 2019 to 2022, he has been a Resource Person/Visiting Professor at the Department of Electronics and Communication Engineering, National Institute of Tiruchirappalli, India, with in the SPARC Project of the Ministry of Human Resources, India. He also works as the Director of Postgraduate and Research with Sri Lanka Technological Campus (SLTC), Padukka, Sri Lanka, and the Founding Head of the Centre of Telecommunication Research, SLTC, since January 2019. He is supervising/supervised ten Ph.D. students and many master's and undergraduate students and three postdoctoral researchers. Since 2022, he has been with the COPELABS, Lusófona University, Portugal. In his career, so far, he has attracted nearly 6M $ research funding from many international grant agencies, such as European Commission, Russian Science Foundation, and Ministry of Human Resource India. He has organized or co-organized more than 30 workshops, special sessions, and IEEE conferences. He has published nearly 200 international peer-reviewed journals, conference papers, and books. His research interests include PHY and NET layer prospective of 5G communications technologies, such as NOMA for 5G, cooperative wireless communications, device to device communications, LDPC codes, and unmanned aerial vehicle.

Prof. Jayakody is a fellow of IET. He has received the Best Paper Award from the IEEE International Conference on Communication, Management and Information Technology (*ICCMIT*), in 2017, and the International Conference on Emerging Technologies of Information and Communications, Bhutan, in March 2019. In July 2019, he received the Education Leadership Award from the World Academic Congress. In 2017 and 2018, he received the Outstanding Faculty Award by the National Research Tomsk Polytechnic University, Russia. He also received the Distinguished Researcher in Wireless Communications, Chennai, India, in 2019. He received the Presidential Award for outstanding research performance, in 2021. He also received the ''Best Publication Award'' at SLTC, in 2019 and 2020. He also serves as an Area Editor for the *Physical Communications* (Elsevier), *Information* journal (MDPI), *Sensors* (MDPI), and *Internet Technology Letters* (Wiley). Also, he serves on the Advisory Board for *Multidisciplinary Science Journal* (MDPI). In addition, he serves as a reviewer for various IEEE Transactions and other journals.